Filled Reactive Ethylene Terpolymer Primers for Cathodic Disbondment Mitigation

C. T. Love,[1] V. M. Karbhari[1,2]

[1]*Naval Research Laboratory, Washington, DC 20375-5342*
[2]*University of Alabama in Huntsville, Huntsville, Alabama 35899*

Received 20 October 2007; accepted 18 March 2008
DOI 10.1002/app.28564
Published online 23 July 2008 in Wiley InterScience (www.interscience.wiley.com).

ABSTRACT: A reactive ethylene terpolymer (RET) with inorganic fillers of clay, talc, and zinc was examined for its cathodic disbondment (CD) performance and as a potential coating primer material for pipeline applications. The filler type and volume fraction influenced the mechanical, thermal, adhesion, and CD resistance of the coatings. The tensile modulus and strength of the RETs increased at higher loadings of selected fillers. The dry adhesive strength of the clay-filled RET maintained the same level of adhesion up to approximately 23 vol %, whereas the talc- and zinc-filled RETs showed decreases in adhesive performance. CD resistance was significantly improved with 18–23 vol % clay, whereas the overall disbondment area was reduced approximately 82% from pure RET. However, the post-cathodic-disbondment adhesive strength for the clay-filled RET decreased as a result of the degradation of the primer/topcoat interface caused by moisture absorption. © 2008 Wiley Periodicals, Inc. J Appl Polym Sci 110: 1531–1544, 2008

Key words: coatings; degradation; fillers; thermoplastics

INTRODUCTION

In excessively corrosive environments, metal structures with organic protective coatings may also require cathodic protection to maintain immunity, such that corrosion reactions are impaired. One can ensure long service lives for coatings used in conjunction with cathodic protection by minimizing moisture diffusion, slowing oxygen and other corrosive species from migrating to the metal surface, and resisting surface scratches. However, in the instance of a damaged coating, even the smallest scratch acts as a cathodic site where oxygen reduction reactions create a highly alkaline environment and facilitate coating disbondment.[1] Cathodic disbondment (CD), or delamination, is the loss of adhesion between an organic coating and a cathodically protected metal substrate due to the electrochemical reduction of oxygen and water at the coating interface. This reaction creates a high concentration of OH^- ions and can raise the local pH above 13.[2,3] As the reaction ensues, covalent, van der Waals, and hydrogen bonds at the polymer/metal interface are weakened and ultimately ruptured.[4] Organic coatings that offer high wet adhesion strength and resistance to saponification often perform well in CD testing.[3]

Correspondence to: V. M. Karbhari (vmk0001@uah.edu).
Contract grant sponsor: DuPont Chemical Co.

Fusion-bonded epoxy primers have been used quite extensively in pipeline applications because of their resistance to CD.[5–7] Although these materials have proven to be successful for many years,[6] thermoplastic polymers may offer significant advantages over thermoset coatings in certain applications where aspects such as time to cure, toughness, and durability are of utmost concern. Thermoplastics may be applied as coatings or primers in various thicknesses in single applications, whereas epoxies must be applied in thin, often brittle layers to build up the requisite thickness; this often leads to concerns related to microcracking, shrinkage, and interlayer adhesion. Additionally, hot-melt thermoplastics eliminate production curing time, offer a more environmentally friendly approach with reduced emissions, and may be applied in the field with a variety of traditional fusion bonding techniques.[8] Historically, the high adhesive strength of thermoplastics has best been established by coatings in the family of ethylene copolymer ionomers, which are ion-neutralized (typically by sodium ions) ethylene methacrylic acid copolymers.[9–11] These materials possess the desired toughness, impact resistance, and adhesion for pipeline coating applications but are sensitive to the permeation of moisture. An olefin (polyethylene) material may be a better choice for such coating applications in wet and corrosive environments.[12]

Inorganic fillers are routinely incorporated into polymers to reduce cost,[13] improve mechanical performance,[13–15] enhance hardness,[13] reduce

TABLE I
Physical Properties of the Inorganic Filling Media

Filler	Chemical name	Molecular formula	Density (g/cm^3)	Particle size (μm)
Clay	Hydrous alumino silicate	$Al_2O_3{\cdot}4SiO_2{\cdot}H_2O$	2.4	~ 20
Talc	Hydrous magnesium silicate	$3MgO{\cdot}4SiO_2{\cdot}H_2O$	2.8	~ 24
Zinc	Zinc	Zn	7.1	2–10

permeability,[16,17] provide extra protection against corrosion of metallic substrates,[3] improve dimensional stability at elevated temperatures,[13,14] improve impact resistance,[13] and protect against UV degradation.[18,19] Hydrous magnesium silicate, commonly known as talc, is commonly added to polymers because of its softness, lubricity, excellent wetting, and ease of dispersion, which may improve the tensile properties of the host polymer.[19] The reinforcing effect offered by talc is due to its platelike structure, which adds rigidity and resists creep even at elevated temperatures. The platelike structure of talc also makes the filler an ideal barricade for reducing the permeability of gases and water vapor.[19]

Hydrous aluminum silicate (clay) is commonly used to increase the tensile strength and modulus of low-glass-transition-temperature (low-T_g) thermoplastics without the sacrifice of elongation and impact performance.[20] Although its layered aluminum silicate structure is hydrophilic and accepts water even after just 1 day of immersion,[21] when dispersed adequately, this mineral filler can provide a permeation barrier against oxygen and water vapor transmission through a reactive ethylene terpolymer (RET).[22] For RET primer coatings with an impermeable topcoat, the diffusion properties through the film are not as important as the ability of the polymer to remain bonded to steel even under harsh corrosive conditions.

The addition of metal powders, specifically zinc, to thermoplastic polymers has been studied for a wide variety of applications, such as the discharge of static electricity, heat conduction, electromagnetic interface shields, and electrical heating.[23] The addition of zinc powder to thermoplastics also provides corrosion protection, where the zinc acts as a sacrificial anode protecting an underlying metal substrate. The electrochemically active nature of the zinc within a polymer primer may help to reduce the amount of O_2 and H_2O reactants that find their way to the primer/metal interface. Reducing the concentration of oxygen at the coating/substrate interface, as in a deaerated electrolyte, has been shown to prevent the escalation of CD.[1]

A RET composed of ethylene/*n*-butyl acrylate/glycidyl methacrylate formulations (Elvaloy 4170, DuPont, Wilmington, DE), by taking advantage of the dual functionality glycidyl methacrylate component, has shown promise in applications such as CD resistance coatings and primers.[12] Mineral fillers added to RET can improve the mechanical cohesive strength and stiffness and further reduce the permeability of the coating by occupying polymer free volume. As a general trend in the literature, going to smaller nanosized diameter fillers with increased exfoliation provides increased resistance to the diffusion of reactive species;[24] however, for the purpose of preventing CD in the primer situation with an impermeable topcoat [ultra-high-molecular-weight polyethylene (UHMWPE)], the material selection of the fillers sis of primary importance.

The objective of this study was to investigate the effect of micrometer-scale clay, talc, and zinc inorganic fillers on the CD resistance of a RET with application for metal coating primers under an impermeable topcoat.

EXPERIMENTAL

Materials

Micrometer-scale fillers of clay (Aldrich, St. Louis, MO), talc (Aldrich), and zinc (ZCA, Monaca, PA) were extrusion compounded into a RET, Elvaloy 4170. The physical properties of the inorganic fillers and the RET resin are shown in Tables I and II, respectively. Platelets sizes of approximately 20–24 μm were selected for the clay and talc materials, whereas the zinc fillers consisted of a random distribution of spherical particles between 2 and 10 μm in diameter. A broad melt temperature range was observed for the pure RET, spanning from 29.5 to 87.0°C, as characterized previously.[25] The elastomeric

TABLE II
Physical, Mechanical, and Thermal Properties of the RET Resin

Polymer	Manufacturer	Melt flow index (g/10 min)	Density (g/cm^3)	E (MPa)	Tensile strength (MPa)	Elongation at break (%)	Melting temperature (°C)	T_g (°C)
Elvaloy 4170	DuPont	8	0.94	5.0	4.5	526	29.5–87.0	−39.8

n-butyl acrylate component of the terpolymer contributed to an elongation at break value of 526%.

Compositional studies were done by the reduction of filler content from master batches to achieve volumetric percentages (samples C4, C18, C23, T3, T15, T23, Z3, Z8, and Z39, where C4 is 4 vol % clay in RET, T3 is 3 vol % talc in RET, Z3 is 3 vol % zinc in RET, etc.) with a reciprocating-screw injection-molding machine. The upper limit for the zinc particles (39 vol %, i.e., 80 wt %) was chosen to coincide with the level used in general compositions for zinc-rich anticorrosion coatings.[3] The composites were injection-molded into tensile dogbone coupons following ASTM 638 type I specifications[26] for mechanical characterization (overall length = 165 mm, gauge length = 50 mm, width of narrow section = 13 mm, and thickness = 3.2 mm). To eliminate the negative effects of absorbed moisture on the quality of the processed coupons, all pellets were dried at 60°C for at least 12 h before injection molding. Three barrel heat zones were held constant at 175°C with the mold was preheated to 40°C to minimize coupon shrinkage. Injection pressures were varied accordingly from 3.1 to 6.2 MPa (450–900 psi) to facilitate differences in filler content. Tensile bar moldings were left to equilibrate to ambient temperature before they were hot-pressed at 215°C under 1 T of pressure over a 232-cm^2 platen area to form films approximately 100–200 μm thick.

Adhesive and CD cell assembly

Clay-, talc-, and zinc-filled polymer films (100–200 μm thick) were cut to 50-mm diameter discs for adhesive and CD testing. Hot-press molding was used for the manufacture of the three-component assembly (steel/primer/topcoat) for CD testing, as shown in Figure 1. The steel (A36 structural grade) side of the assembly was heated and held at a constant temperature of 215°C, whereas the bottom platen was held at room temperature to minimize warpage of the rigid UHMWPE polymer substrate. Lower molecular weight polymer interdiffusion occurring at the UHMWPE/primer interface created a semiinfinite bond such that the UHMWPE/polymer bond was strong enough so that during the adhesive pulloff test, the measured quantity was the level of adhesion at the steel/primer interface. The assembly was kept within the platens under minimal pressure for 5 min to ensure the complete melting of the composite film. Next, the assembly was removed from the press and left to cool to room temperature (23°C). An artificial defect of diameter of 6.35 mm ($^1/_4$ in.) was drilled through the UHMWPE topcoat and the RET primer to expose a clean steel surface.

In a previous study, the use of a silane pretreatment for steel enhanced the CD performance of RET and RET/high density polyethylene blend coatings.[12] The silane coupling agent was applied to grit-blasted steel before the hot-press bonding step. For simplicity, only a single silane concentration of 0.4 vol % γ-aminopropyltriethoxysilane in a 1 : 1 ethanol/water solution was applied on the basis of an initial study of concentrations ranging from 0.1–3.0 vol %. The silane/ethanol/water solution was brushed on the metal surface and allowed to dry for at least 3 h at 23°C before bonding.

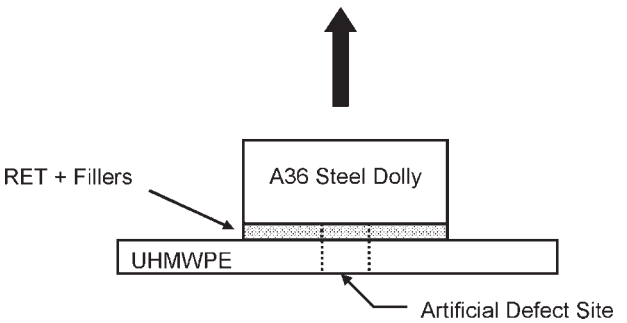

Figure 1 Bonding schematic of RETs with fillers for the primer between the ultra-high-molecular-weight substrate and A36 steel dolly.

Tensile testing

Tensile testing was performed according to ASTM D 638.[26] The extension rate was 50 mm/min, and all tests were performed at 23°C. Five samples were tested for each blend composition with average properties reported. The stress–strain behavior for all of the materials was elastic–plastic, and the modulus of elasticity was calculated from the initial linear elastic region.

Dry adhesive pulloff

The adhesive pulloff strength was measured with a portable pulloff tester following ASTM D 4541-02.[27] Structural grade A36 steel dollies 50 mm in diameter were sandblasted and bonded to 3.18 mm thick UHMWPE ($E \sim 680$ MPa, tensile strength (σ_{ts}) ≈ 40 MPa) substrates with the filled RET as an adhesive (as shown in Fig. 1). UHMWPE was chosen because its nonconductive nature would not disrupt CD testing, and a resistance to thermal deformation up to 150°C allowed it to be used in hot-press bonding.

CD/adhesion testing of the filled thermoplastic primers

A test fixture was developed to measure the combined pulloff adhesion/CD performance of the filled RET primers with a steel dolly both as the metal cathodic substrate and pulloff adhesion disc, as shown in Figure 2. CD parameters, voltage and electrolyte,

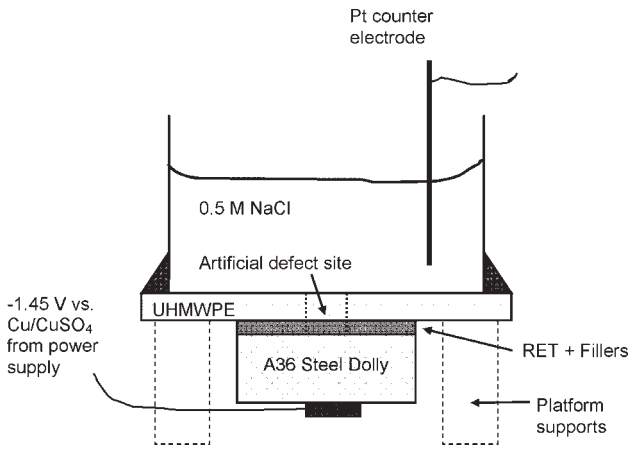

Figure 2 Schematic of cell for CD testing and post-CD adhesive pulloff for the clay-, talc-, and zinc-filled RET primer coatings.

were based on ASTM G8-96[28] standards with slight modifications. An imposed cathodic potential of −1.45 V versus $Cu/CuSO_4$ was applied in a 0.5*M* NaCl electrolyte at 23°C with a platinum wire anode for 840 h (5 weeks). Care was taken to monitor and correct fluctuations in the cathodic potential as the severity of the CD area is greatly affected by changes in voltage.[29] After the designated CD testing period, a steel bolt was threaded into the dolly to the full bore depth of 0.5 in., and the assembly was tested with a portable pulloff tester. This situation mimicked an adhesive tie layer where an impermeable topcoat was assumed with only the defect (diameter = 6.35 mm) being in contact with the electrolyte solution. The CD area was measured (we subtracted the area of the initial artificial defect) after destructive adhesive pulloff testing where the radial disbondment could easily be seen without magnification.

Dynamic mechanical thermal analysis

A Rheometric Scientific dynamic mechanical thermal analyzer with a tensile fixture was used to determine the viscoelastic properties of the primer films. Film specimens were tested with a gage length of 10 mm from −100 to 50°C at 3°C/min at a frequency of 1 Hz and a prestrain of 0.001. Liquid nitrogen was used to achieve subambient temperature. Values for T_g for each specimen were taken from the peak of the tan δ curve, where tan δ is the ratio of the loss modulus (E'') to the storage modulus (E').

Moisture uptake characterization

To understand the hydrophilic/hydrophobic effects of the clay, talc, and zinc fillers in the RETs, moisture uptake testing was conducted at room temperature in a 0.5*M* NaCl solution for 696 h to mimic the concentration and type of electrolyte used in CD testing. Before immersion, the 50-mm diameter primer films (thickness ≈ 330 μm) were dried in a 60°C oven for 12 h to remove any previously absorbed moisture. Once immersed, the films were periodically removed, patted dry to remove excess moisture, weighed, and placed immediately back into the solution bath. The mass was recorded in terms of percentage mass gain.

RESULTS AND DISCUSSION

Scanning electron micrographs of the impact freeze fracture surfaces are given in Figure 3. The clay filling media agglomerated into clumps, whereas talc remained as well-dispersed platelets. The zinc fillers showed a uniform dispersion and separation of various diameter particles throughout the RET matrix. Dispersion compounding in this study was done via a reciprocating-screw injection molder. It was reasonable to assume that a more advanced method for compounding, such as extrusion, would yield a better dispersion of the fillers in RET.

The fracture surfaces of the clay-filled RET suggested the propagation of crack growth through ductile clay particles. The residual clay particles appeared to be sheared, where the cracks migrated directly through the filler [Fig. 4(a)]. Talc-filled RET, on the other hand, indicated only limited interaction between the polymer and the filler, as evident by the delamination failures surrounding the rigid talc platelets [Fig. 4(d)] and the platelet-shaped voids talc particles once occupied [Fig. 4(e)]. The failure appeared more brittle as the composition of talc was increased to T23 [Fig. 4(f)], where the jagged but flat fracture surface indicated a lack of ductile deformation. The interface at the RET/zinc interface appeared to be the strongest where the metal spheres deflected crack growth and left a thin coating of polymer over the filler surface to encapsulate the particles, as shown in Figure 4(g). The appearance of ridges along the fracture surface for Z3 [Fig. 4(h)] indicated some degree of ductile failure. As the zinc content increased, the fracture surfaces showed a transition from ductile failure (Z8) to more brittle failure [Z39; Fig. 4(i)]. A comprehensive study of particle-filled thermoplastic polyesters done by Li et al.[30] schematically illustrated the modes of fractography with increasing volume percentage of calcium terephthalate and calcium carbonate. Using the Li et al. fracture surface designations as a reference, several conclusions were drawn regarding the fracture surfaces of the clay-, talc-, and zinc-filled RET in this study. As expected, the most ductile fracture surface was seen in the unfilled elastomeric RET. A similar surface was seen in Z3, where void formation and

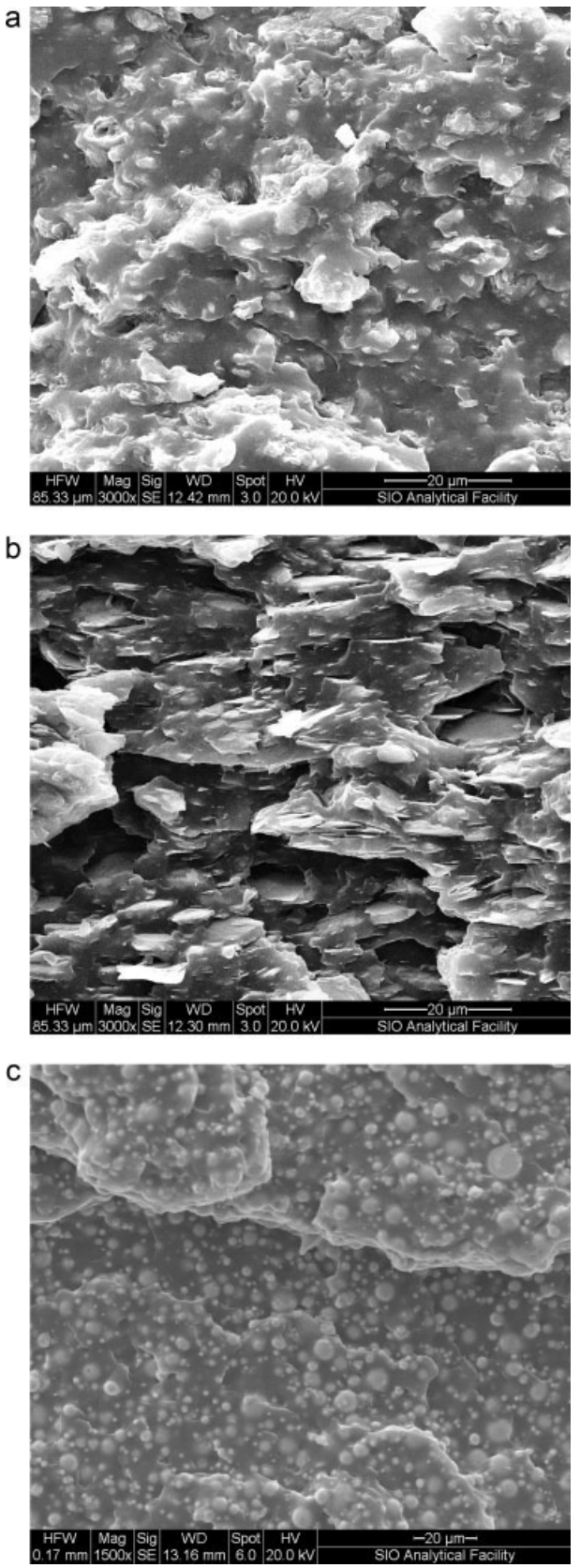

Figure 3 Scanning electron micrographs of the impact freeze fracture surfaces identifying the mode of failure and content, dispersion, and separation of the (a) clay, (b) talc, and (c) zinc fillers in RET.

growth around the zinc particles caused splitting and tearing of the host RET, which ultimately led to a ductile tearing fracture. For low volume percentage fillers in RET (C4, T3, Z8), a slightly different fracture mode was evident but was still classified as ductile failure. For these composites, C4, T3, and Z8, fracture was driven by the coalescence of voids surrounding the inorganic particles. This was similar to RET and Z3; however, in this case, the voids merged laterally until they ultimately reached some critical size flaw where tearing ensued until rupture. As the filler contents increased to C18 through C23, T15 through T23, and Z39, the fracture surfaces indicated a transition from ductile to quasibrittle fracture, where an increase in filler content led to an increase in void formation surrounding the particles. The high concentration of particles (voids) placed high local stress on the thin polymer segments between the particles. When the thin segments were no longer able to carry load, a lateral coalescence of voids took place, which led to a more brittle fracture surface.

Mechanical and thermal properties of the filled RET

The elastic modulus (E), strength, and elongation at fracture were measured via tensile testing. The stress–strain behavior of all of the composites was completely elastic–plastic at 23°C. The addition of inorganic fillers improved the E value of the RETs at higher loadings. At low filler contents (samples C4, T3, and Z3), no significant improvements in the tensile modulus over that of the unreinforced RET ($\sim$ 5 MPa) were seen, as shown in Figure 5. T23 offered the greatest enhancement in stiffness, a 533% improvement over the unreinforced RET. The addition of clay particulate fillers provided increased stiffness up to 270% at a near linear rate as the filler content increased to C23. The addition of zinc increased E only slightly from 3 to 8 vol %. Above 8 vol %, the modulus increased sharply from 5.8 to 23.3 MPa for Z8 and Z39, respectively, which provided an increased stiffness 366% higher than the unreinforced RET. The stiffness increases offered by the addition of inorganic fillers in the RET may be attributed to percolation theory, as outlined by He and Jiang,[31] where under applied tensile load, stress concentrations arise around the fillers and cause a plane-strain-to-plane-stress transition in the polymer matrix material surrounding the filler. He and Jiang assumed that all particles are spherical and that particle sizes remain somewhat constant, such that the interparticle distance between the filler particles decreases with increased weight fraction of the filler. Thus, as the filler content is increased in the polymer, the number of percolation pathways formed

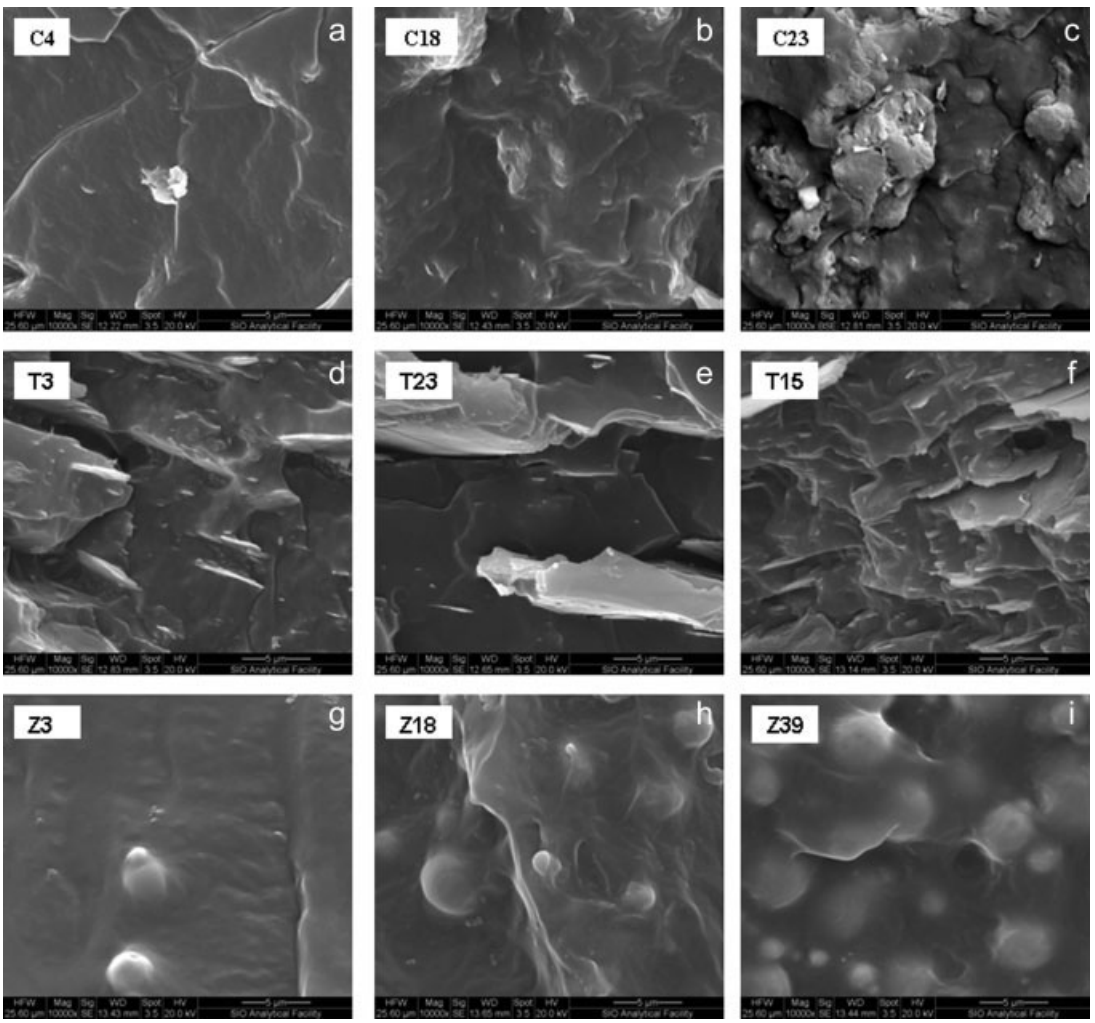

Figure 4 Freeze impact fracture surface of RET with inorganic fillers illustrating the particle geometry and particle/matrix interaction. The clay-filled RETs, (a) C4, (b) C18, and (c) C23, showed modest polymer/particle interaction, as evident by particles shearing. The talc-filled RETs, (d) T3, (e) T15, and (f) T23, showed rigid platelet particles delaminating from the host polymer to leave inclusion-shaped voids. The zinc-filled RETs, (g) Z3, (h) Z18, and (i) Z39, showed high levels of polymer/particle adhesion where the fracture surfaces showed a thin layer of polymer bound to the spherical zinc particles.

cause a rapid increase in the composite E.[31] In this study, the clay and talc fillers existed as platelets, as shown in Figure 4(d–f), whereas zinc particles were spherical with a distribution of particle diameters between 2 and 10 μm. To help define a mechanistic model for modulus behavior with added inorganic fillers, the modulus was plotted against the filler volume fraction (Fig. 5). Under the given assumptions, the Halpin–Tsai (rigid platelet fillers) and Lewis–Nielson (spherical particles with designated packing factors) models corresponded well to the experimental data as shown, especially at higher loadings. Table III shows the correlation of actual experimental data taken from tensile testing with the predicted values at given filler volume fractions. The platelet clay and talc particles added to RET acted much like short fibers with aspect ratios (length/diameter) and, thus, correlated with a fair degree of accuracy with the Halpin–Tsai model,[32–34] where the modulus of the composite (E_c) is calculated as follows:

$$E_c = E_m \times \frac{1 + ABV_f}{1 - BV_f} \tag{1}$$

where V_f is the volume fraction of fillers.

$$A = 2(l/d) \tag{2}$$

and

$$B = \left(\frac{E_f}{E_m} - 1\right) \Big/ \left(\frac{E_f}{E_m}\right) + A \tag{3}$$

where E_m is the modulus of the matrix resin, E_f is the modulus of the fiber (the rigid platelet filler in the

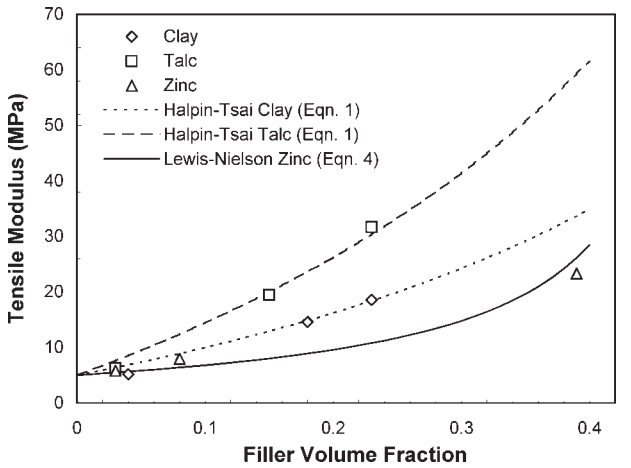

Figure 5 Effect of the inorganic fillers and loading on E values of RET specimens pulled in tension at 50 mm/min at 23°C.

current investigation), l is the length of fiber or platelet ($l_{clay} = 20$ μm, $l_{talc} = 24$ μm), and d is the diameter or thickness of the fiber or platelet ($d_{clay} = 5$ μm, $d_{talc} = 3$ μm) based on manufacturer specifications and scanning electron microscopy observations.

The model developed by Lewis and Nielson[35] for E of filled polymers includes a maximum packing fraction term, which corresponded well with the experimental data for spherical randomly sized zinc particles in RET. In the Lewis–Nielson model[35]

$$E_c = E_m \times \frac{1 + ABV_f}{1 - B\psi V_f} \tag{4}$$

where

$$\psi = 1 + \left(\frac{1 - \phi_{max}}{\phi_{max}^2}\right) V_f \tag{5}$$

where ϕ_{max} is the maximum packing factor and is 0.52 for simple cubic geometric packing.[36] The Halpin–Tsai and Lewis–Nielson models corresponded well with the experimental data as shown, especially at higher loadings.

No significant changes were seen in the tensile strength between the unreinforced RET (4.50 MPa) and the samples with the lowest filler contents: C4 (4.07 MPa), T3 (4.52 MPa), and Z3 (4.24 MPa). The ultimate tensile strength improved linearly thereafter with the addition of all three filler materials (Fig. 6). Talc and zinc fillers at the highest loadings (samples T23 and Z39) provided increases in strength of 48 and 23%, respectively. Clay-filled RET was observed to be strongest for sample C18 (38% increase) rather than for sample C23 (34% improvement), but this could have very well been due to scatter and local variation in filler distribution.

The elongation at fracture of the filled RET primers decreased with increasing filler content. Plotting elongation as a function of filler volume fraction, as shown in Figure 7, yielded a better illustration of the changes in fracture behavior at higher loadings. The addition of zinc particles resulted in the highest loss in elongation at fracture (−72%). Clay showed the least affect of filler content on elongation (−52%). A sharp drop in elongation was observed for the talc-filled RET at filler contents greater than that of sample C4. At concentrations higher than that of sample T15, the fracture strain decreased at a much slower rate with increasing filler loading. The decreased elongation at break (up to 86%) at high bentonite (clay) loading (20–50 wt %) was also observed by Othman et al.,[21] who suggested that it was due to the decreased deformability of a rigid filler/polymer interface, whereas at higher loadings, the filler/polymer interactions are replaced by filler/filler interactions.[37] This was confirmed with the ductile particle fracture observed for C23 and shown in Figure 4(c). The clay- and talc-filled RETs studied here showed a transition in elongation behavior between $0.14 \leq V_f \leq 0.22$. The sharp decrease in strain-to-failure existed up to

TABLE III
Experimental Value of E Versus Filler Content for the Clay-, Talc-, and Zinc-Filled RETs and Predicted Values from the Halpin–Tsai [eq. (1)] and Lewis–Nielson [eq. (4)] Models of E of the Particle-Filled Composites as a Function of the Filler Volume Fraction

Filler	Volume fraction	Experimental value (MPa)	Halpin–Tsai model [Eq. (1); MPa]	Lewis–Nielson model [Eq. (4); MPa]
Clay	0.04	5.16 ± 0.45	6.87	—
Clay	0.18	14.59 ±1.32	14.86	—
Clay	0.24	18.59 ±0.96	19.18	—
Talc	0.03	6.2 ±0.67	7.63	—
Talc	0.15	19.43 ±1.37	20.00	—
Talc	0.24	31.66 ±1.79	31.84	—
Zinc	0.03	5.8 ±0.23	—	5.39
Zinc	0.08	7.99 ±1.67	—	6.38
Zinc	0.39	23.3 ±2.04	—	26.17

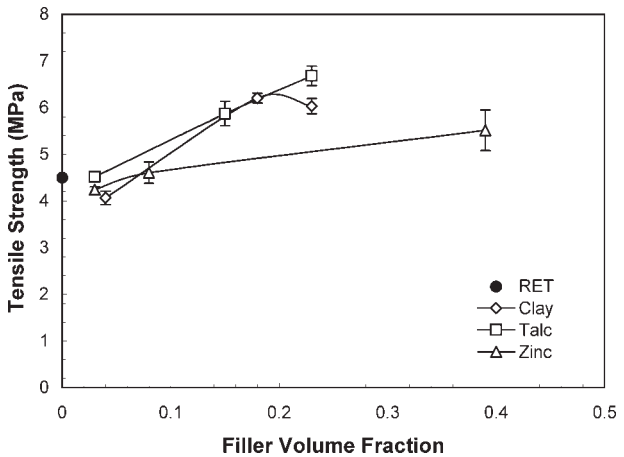

Figure 6 Effect of the inorganic filler type and loading volume fraction on the tensile strength of RET resins pulled in tension at 50 mm/min. The transition from ductile to quasibrittle failure at approximately $V_f = 0.14$ is illustrated by the vertical line.

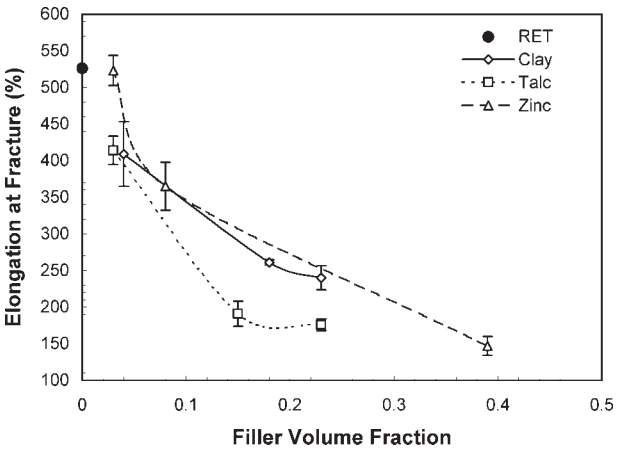

Figure 7 Effect of the inorganic filler type and loading on the elongation at fracture of RET resins pulled in tension at 50 mm/min.

approximately $V_f = 0.14$ for the talc-filled RET. At loadings above 0.14 volume fraction, the elongation behavior remained near asymptotic. This value was in agreement with others reported for talc-filled polymer systems (Li et al.[28] found the threshold value for filler loading (V_{critical}) = 0.14) and elsewhere[21,39] in the literature ($0.10 < V_{\text{critical}} < 0.50$). The transition near $V_f = 0.14$ signified a change from ductile to quasibrittle behavior. This behavior was confirmed by observations discussed previously of the fracture surfaces in the tensile testing of the filled RET materials.

No significant changes were observed for the T_g's, as illustrated in Table IV. The T_g values all fell within the ±2°C sensitivity of the dynamic mechanical thermal analysis. Increasing T_g with filler content would have indicated that particle/polymer interactions increased the internal friction of the composite and hindered the movement of polymer molecules, which would have resulted in a higher value for T_g. A slight initial decrease in T_g was seen for clay and zinc before an increase with higher filler loadings. The study of particle-filled polymers has shown that an increase in filler content results in a similar shift toward higher T_g temperatures.[40] Polymer boundaries encapsulating each particle further decrease the molecular mobility where the T_g of filled polymers is linearly dependent on the volume fraction of the polymer in the boundary layer.[40] The height of the tan δ peak decreased with increasing filler content, which suggested the restriction of molecular motion at high filler contents, with the exception of zinc-filled RET, where a slight increase in the tan δ peak was observed from Z3 to Z8 followed by a large decrease in height from Z8 to Z39. At similar loadings (e.g., C23, T23, Z39), E' was enhanced with a larger, more coarse filler as in T23 (refer to Table I for the particle dimensions), which has also been observed in other inorganic-particle-filled polymers.[41] The E' values for the filled RET primers taken at 23°C (Table IV) correlated with the trends shown by tensile testing at room temperature (Fig. 5). The higher magnitude of E' over E was most likely the result of the additional compression-molding processing step and the effects of the dimensional

TABLE IV
Thermal Properties, T_g, Tan δ Peak Height, and E' and E'' at 23°C, for the Pure RET Resin and RETs with Inorganic Fillers (Clay, Talc, and Zinc)

Sample	T_g (°C)	Peak tan δ (E''/E')	E' at 23°C (MPa)	E'' at 23°C (MPa)
RET	−30.1	0.328	9.46	1.76
C4	−31.2	0.363	18.66	1.19
C18	−29.4	0.329	39.18	2.80
C23	−29.5	0.309	59.75	3.67
T3	−29.3	0.354	19.64	1.47
T15	−26.7	0.330	59.25	4.28
T23	−27.7	0.320	91.90	6.65
Z3	−32.0	0.375	17.19	1.07
Z8	−30.7	0.380	26.45	1.47
Z39	−28.2	0.312	61.12	4.48

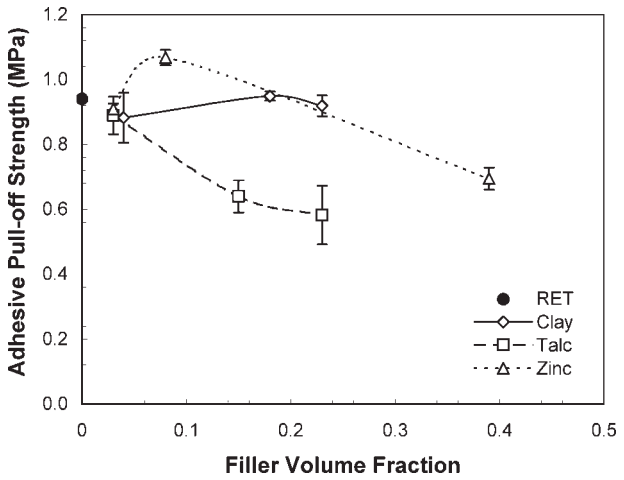

Figure 8 Adhesive pulloff strength of the RET and RETs with inorganically filled primers between the UHMWPE substrate and A36 steel dollies 50 mm in diameter.

differences between the ASTM D 639 type I tensile bars used to calculate E and the thin films used to calculate E'.

Dry pulloff adhesion

The ability of the primer composite to bond both with the UHMWPE substrate and the steel dolly dictated the overall adhesive tensile pulloff strength of the film. The adhesive values shown in Figure 8 along with visual observations of the steel dolly shown in Figure 9(a–c) were necessary to determine the failure mechanism of the primer. *Adhesive failure* was defined here as the loss of adhesion on a surface or substrate where little or no residual polymer was left after complete separation. Conversely, *cohesive failure* was defined as the loss of bond as a result of the internal rupturing of the RET film joining the

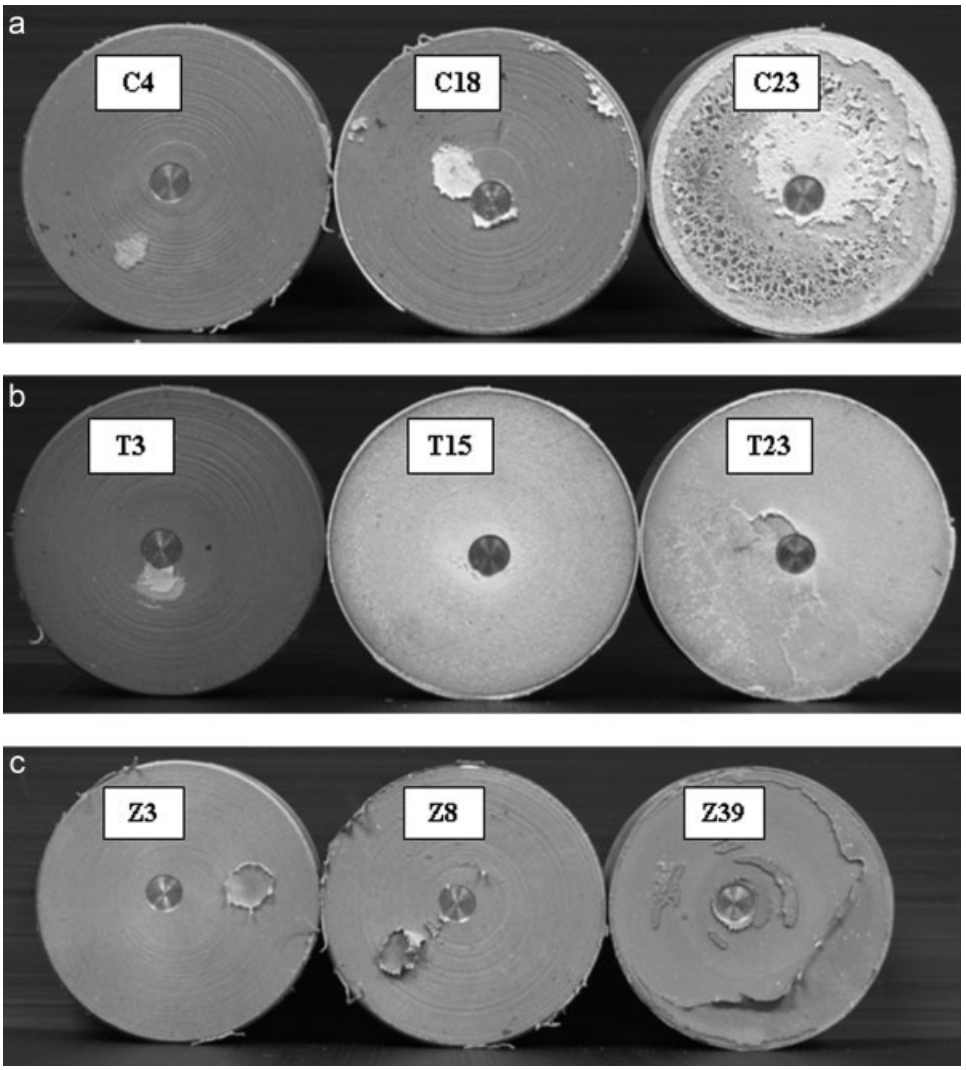

Figure 9 Dolly surfaces after destructive adhesive pulloff testing illustrating the degree of cohesive failure indicated by the amount of residual polymer remaining on the steel surface for the (a) clay-, (b) talc-, and (c) zinc-filled RET primers.

dolly and UHMWPE substrate. Surface analysis has proven useful for determining the locale of failure, whether adhesive, cohesive, or mixed adhesive/cohesive.[3] It is important to keep in mind that there were two interfaces present in the pulloff adhesion assembly used in this study: (1) the steel dolly/primer and (2) the primer/UHMWPE.

After destructive pulloff, the amount of residual polymer remaining on the metal and polymer topcoat surfaces was qualitatively and visually observed to determine the failure and fracture mechanisms. The amount of residual material remaining on the UHMWPE substrate increased with clay filler content, whereas the adhesive strength remained relatively constant: 0.88 MPa (C4), 0.95 MPa (C18), and 0.92 MPa (C23). At lower loadings (C4), adhesive failure occurred at the steel interface with only 1% polymer remaining on the UHMWPE surface [Fig. 9(a)]. The amount of polymer on the UHMWPE surface increased for C18, with only minimal amounts on the steel surface (5%). At highest loading (C23), the primer failed completely cohesively, as evident by the tearing and peeling failure shown in Figure 9(c) (C23), where both the steel and UHMWPE surfaces were completely covered with polymer. At this composition, there appeared to be a very tight bond at the primer/UHMWPE interface, which could have indicated the interdiffusion of lower molecular weight species.

As talc filler was added to RET, the adhesive strength decreased from 0.94 MPa for pure RET to 0.58 MPa for T23, a loss of 38%. The amount of residual polymer on the UHMWPE surfaces for the talc primers remained approximately constant throughout all of the compositions, as determined by visual observation. T3 displayed adhesive failure at the primer/steel interface, whereas T15 and T23 failed as a result of cohesive rupture [Fig. 9(b)]. The failure displayed in Figure 9(b) (T23) showed delamination within the composite film as a source of failure. A possible explanation for this cohesive failure is that it was the result of imperfections within the primer or stress concentrations surrounding the inorganic fillers, which initiated cracks that were furthered under tensile pulloff load.

Like the clay-filled RET, zinc-filled RET displayed increased residual polymer at the primer/UHMWPE interface as the filler content increased. Again, at low filler content (Z3), failure was almost entirely adhesive where the primer did not remain bound to the steel surface. As zinc levels increased, the failure mode shifted from mixed adhesive/cohesive (Z8) to fully cohesive (Z39). The highest adhesive strength of 1.07 MPa for Z8 correlated to the mixed mode peel/tear failure, as shown in Figure 9(c). The adhesive pulloff data along with visual observations suggested that the highest strength against pulloff for the filled RET primers between the steel and UHMWPE surfaces depended on both the tensile and adhesive properties of the composite. It is important to point out that under cohesive failure, all that is known about the actual adhesive strength, however, is that it is greater than the measured value.[3]

CD performance of the clay-, talc-, and zinc-filled RET primers

The application of cathodic potential prevented the artificial defect from corroding even when it was in contact with a 0.5*M* NaCl solution for 840 h (5 weeks) for all of the specimens. However, the electrochemical reduction of oxygen and the dissociation of water at the defect site created a severe environment, which led to the disbondment of the RET and filled RET primers surrounding the initial defect. The disbondment areas could easily be calculated after adhesive pulloff testing. After pulloff, a small amount of water was observed under all of the disbonded films at the primer/steel interface, which indicated an ingress of moisture along the disbondment front. Nearly all of the samples tested displayed a near-perfect circular disbondment pattern, as shown in Figure 10. In the few instances of irregular disbondment geometry, average disbondment radii were taken to calculate the average area of CD. Figure 11 shows the average CD area (minus the initial defect area) of five samples tested for each composition. Clay-filled RET provided the greatest reduction in CD area, approximately 82% for C18 and C23. No changes in disbondment area were noticed in the talc- and zinc-filled RETs at low loading. A modest reduction of 8.6% in CD area was seen at the highest level of talc loading (T23). This value was slightly lower than that observed by Roy et al.,[42] who found that with the addition of 10 wt % talc filler ($\sim$ 3 vol %) to medium-density polyethylene coatings, the CD radius decreased from 20.8 to 14.3, a 50% reduction in CD area. Roy et al.'s increased resistance to CD was attributed to increased dry bond strength due to the reduction of thermal shrinkage after processing with the addition of talc. For this study, several conclusions about dry adhesive pulloff strength and CD performance were drawn. First, the CD resistance was highest for the clay-filled RET, where the adhesive integrity remained relatively constant from C3 through C23 (Fig. 8), near that of the unfilled RET. This suggested that the dry adhesive strength assisted in resisting CD via mechanical means; however, other characteristics may have more heavily influenced the overall CD protection offered by the primer, such as durability in electrochemical cells, moisture uptake, and wet adhesive strength. Second, the addition of talc

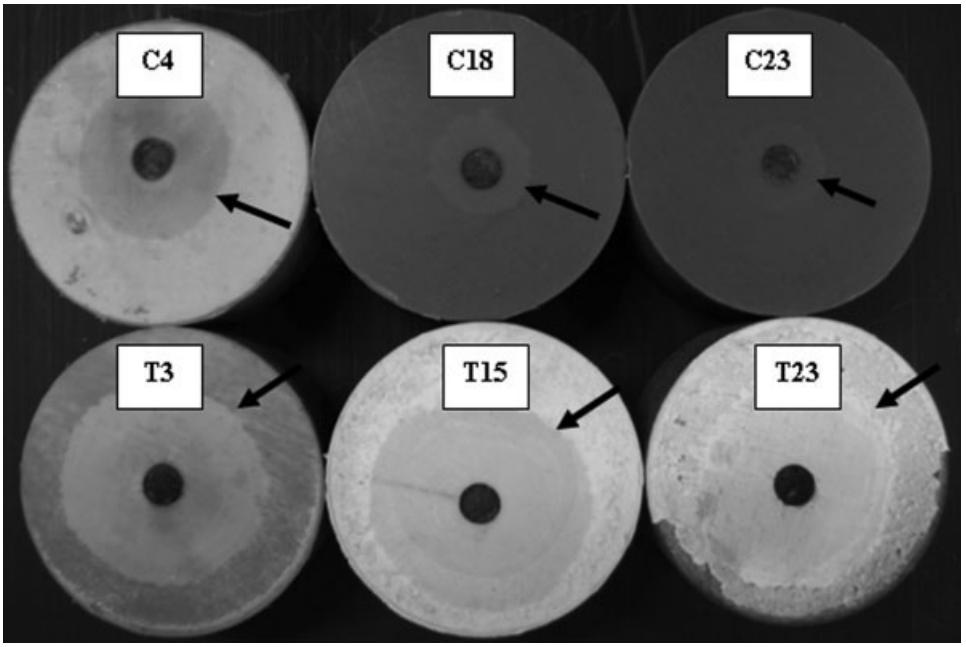

Figure 10 Steel dolly surfaces illustrating the pulloff fracture surfaces and disbondment areas for C4, C18, C23, T3, T15, and T23 after 840 h under CD testing. The outer disbondment radii are noted by arrows.

to RET created a loss in adhesive performance coupled with only minimal protection against CD at high filler volume fractions (T23).

The incorporation of zinc particles increased the overall CD area by 27.8% at Z8. However, at the highest level of zinc added (Z39), the CD area was decreased 24.6%, which was most likely the result of zinc particles behaving as diffusion barriers and resisting moisture uptake and ionic mobility than electrochemical reactions taking place within the coating instead of at the primer/steel interface. The overall performance of the zinc-filled RET supported the notion that a nonconductive primer may be necessary to minimize the effects of CD, which was explained elsewhere.[1]

Post-cathodic-disbondment (post-CD) adhesion of the filled RET

The initial dry and post-CD adhesive strengths for the filled RET primers are given in Table V. A tremendous loss of adhesive strength between 52 and 85% of the original dry pulloff adhesive strength was observed for clay-filled RET, whereas adhesive losses in the talc- and zinc-filled RETs were within 5–12 and 6–31%, respectively, of dry condition measurements and followed the same trends as under the initial conditions. The clay-filled RET primers, however, behaved completely different, where a continual loss in adhesive strength was evident as the filler content increased. One explanation for the drastic changes in adhesive performance could be that they were the result of moisture diffusion into the primer layer from the exposed defect site. Moisture absorption measurements were taken at conditions similar to the CD testing regime (solution concentration, temperature, and immersion time). During CD testing in the primer situation described previously, moisture was only permitted to enter the primer laterally from the defect site. Moisture absorption testing consisted of free-standing films exposed to a 0.5*M* NaCl solution at 23°C for 696 h, which yielded a total exposed surface area of 3927 mm^2. After the immersion time in solution, large volume increases (~ 25%) due to swelling were observed for the clay-filled RET (C23). The moisture

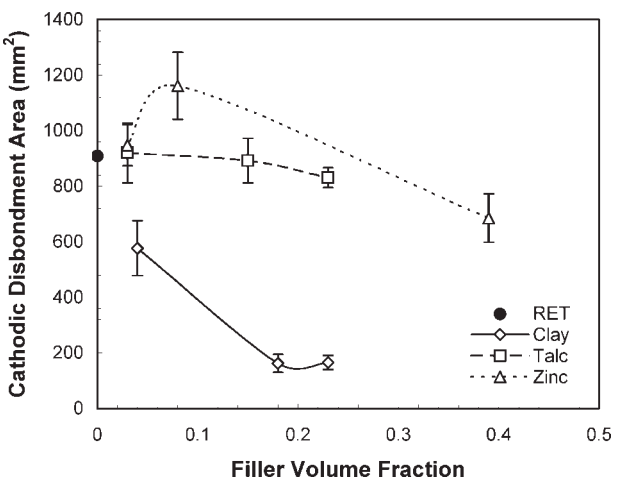

Figure 11 CD areas for the RET primer coatings on steel with the clay, talc, and zinc fillers at various compositions after 840 h (5 weeks) of testing at −1.45 V versus $Cu/CuSO_4$ in 0.5*M* NaCl at 23°C.

TABLE V
Adhesive Pulloff Strength of the RET and Inorganic Clay-, Talc-, and Zinc-Filled RET Under Initial Dry Conditions and After the 840-h CD Period with the Magnitude of the CD Area Given as a Reference

	Adhesive pulloff strength (MPa)		
Sample	Initial	Post-CD	CD area (mm^2)
RET	0.94	0.88	909
C4	0.88 ± 0.08	0.42 ± 0.06	577 ± 99
C18	0.95 ± 0.01	0.14 ± 0.02	162 ± 32
C23	0.92 ± 0.03	0.18 ± 0.04	166 ± 26
T3	0.89 ± 0.06	0.79 ± 0.22	920 ± 108
T15	0.64 ± 0.05	0.59 ± 0.15	892 ± 80
T23	0.58 ± 0.09	0.55 ± 0.01	831 ± 36
Z3	0.91 ± 0.02	0.63 ± 0.32	948 ± 74
Z8	1.07 ± 0.02	1.00 ± 0.01	1162 ± 121
Z39	0.69 ± 0.03	0.69 ± 0.27	685 ± 87

uptake of filled polymer adhesives has been described to be a result of one or a combination of two mechanisms: (1) water molecules accumulating and migrating within the apparent free volume of the polymer and (2) water uptake through the formation of hydrogen bonds within the polymer, which immobilize the water and cause swelling.[43] No dimensional changes were detected for T23 or Z39. The swelling observed for the clay-filled RET was most likely due to the hydrophilic nature of the clay filling media rather than the adsorption characteristics of the unfilled polymer. A plot of moisture (0.5*M* NaCl) absorption versus immersion time is shown in Figure 12, where M_t is the percentage mass moisture absorption at time t (h). The magnitude of moisture uptake for clay (C23) was 10.25% at 696 h. This was two orders of magnitude greater than the M_t values for talc (T23) and zinc (Z39), which were 0.16 and 0.57%, respectively. The rate of moisture absorption began very rapidly for clay and then leveled out after 300 h, which indicated near-complete saturation. The rate of moisture absorption for Z39 remained linear up to 696 h of immersion. The bentonite clay used in this study was naturally hydrophilic and remained such when it was added to the RET resin.

Complete adhesive failure at the primer/UHMWPE interface was observed for all clay-filled RET primers as well as T3 and Z3. This was in direct contrast to the adhesive behavior of the clay-filled primers under dry conditions, where cohesive failure was most commonly observed as indicated by high levels of residual polymer remaining on the UHMWPE surface after separation. At higher talc and zinc loadings, the failure mechanism shifted from adhesive at the primer/steel interface to completely cohesive within the primer. Large standard deviations were observed for the talc-filled RET, whereas virtually no deviations were observed with the zinc-filled RET. The high adsorptive capacity of talc has been theorized elsewhere[18] to absorb low-molecular-weight species generated during the thermal cycling of thermoplastic coatings (the lamination process) that occurs during the coating process, which thereby improves the cohesive film strength and adhesion at the interface of steel and polyethylene.[42] However, zinc is hydrophobic and can help resist the absorption of moisture along the defect interface, therefore maintaining the mechanical and physical integrity of the primer film. As a general observation, a large amount of plastic deformation was found in films with filler contents of 8 vol % or greater, whereas higher modulus primers (at higher loadings) did not yield as extensively before failure.

According to the data in Table V, no direct relationships were observed among the adhesive strength, wet adhesive strength, and CD performance of the clay-, talc-, and zinc-filled RET primers. It has been suggested[44] that dry adhesive strength can be an indicator of CD performance, but this was not the case for the materials examined in this study. The findings of Harun et al.[45] suggest that CD may be controlled by the interfacial processes of hydrolysis and bond scission for epoxide coatings or by hydrolysis and bond scission within the bulk polymer for alkyd coatings. Although interfacial degradation may be the mechanism for CD of epoxide-containing RET primers, degradation of the polymer bulk as a result of moisture absorption must also be considered. The post-CD adhesive pulloff surfaces for the clay-filled RET (Fig. 10) showed adhesive failure (hydrolysis) at the primer/UHMWPE. This interfacial failure was most likely due to the uptake of moisture, where moisture could degrade the bonds at the primer/UHMWPE interface, either by hydrolysis or by mechanical shearing as a result of swelling

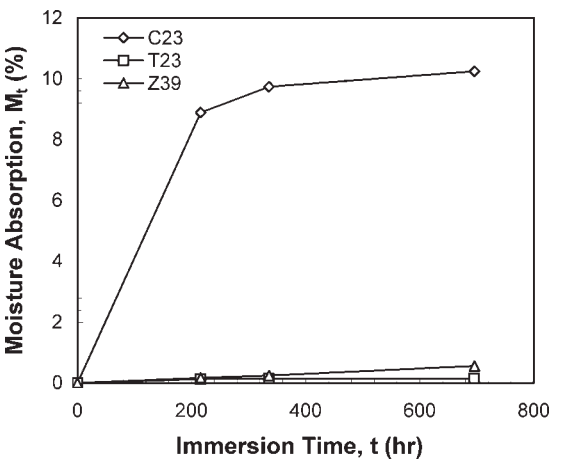

Figure 12 Moisture absorption curves for the free-standing inorganically filled RET films in 0.5*M* NaCl at 23°C with 3927 mm^2 of total exposed surface area (two-sided films 50 mm in diameter).

strains associated with absorbed moisture. For the talc-filled RET primers shown in Figure 10, the rate of hydrolysis of bonds at the primer/steel interface was faster, as indicated by the increased magnitude of CD. Cohesive failure also assumes that some hydrolysis may take place within the bulk polymer, but most importantly, a high level of adhesion is maintained at the primer/topcoat interface. With regard to the coating system adopted in this study, the integrity of the primer/topcoat bond greatly determines the adhesive strength after CD testing; whereas the CD performance was due to the rate of bond degradation at the primer/steel surface. The highest level of protection against CD was, therefore, achieved by the incorporation of clay fillers in the epoxide-containing thermoplastic primer. For overall CD and adhesive performance in a multiple-layer coating systems, the adhesive strength at the primer/topcoat surface must be improved for clay-filled RET.

CONCLUSIONS

The magnitude of CD of a RET may be decreased with the addition of an inorganic filling media: clay, talc, or zinc. A transition in the elongation at fracture behavior from ductile to quasibrittle was observed when approximately 14 vol % platelet clay and talc reinforcing fillers were added to the RET. The transition to quasibrittle fracture was accompanied by a drop in the fracture strain, which caused a loss of toughness that may exclude the application of highly filled RET primers from low-temperature environments. The highest protection of CD was found in clay-filled RET and was dependent on filler content. At clay contents between 18 and 23 vol % in RET, the CD area was reduced approximately 82%. No specific correlations were found between the tensile and adhesive properties with the CD performance of the primers. However, a mixed-mode adhesive/cohesive failure was observed to yield the highest adhesive strength. The post-CD adhesive performance of the talc- and zinc-filled primers followed the same trends observed for ambient adhesion with lower magnitudes. Post-CD adhesion for the clay-filled primers was significantly lower than that under dry conditions, where complete adhesive failure was observed at the primer/UHMWPE. The loss of post-CD adhesion of clay-filled RET suggests that water migration from the defect site along the primer/UHMWPE interface weakened bonds, even when the bond strength was maintained at the primer/steel interface. The moisture absorption data suggested that the clay-filled RET behaved in a completely hydrophilic fashion by absorbing 10.25% of its original mass in only 696 h of immersion in a 0.5*M* NaCl solution at 23°C. The absorbed moisture caused the destruction of the primer/UHMWPE interface and, thus, decreased the overall adhesive strength of the primer/steel/UHMWPE coating assembly. However, the integrity of the primer/steel interface was maintained, and the underlying steel substrate was protected against corrosion and CD, which makes the clay-filled RET a potential primer for dual or trilayer organic coating systems for steel with cathodic protection.

The authors thank DuPont Chemical Co. for financial support and donation of materials for this study. The authors also thank Guijun Xian for his assistance with impact measurements and many helpful discussions, Evelyn York at the Unified Laboratory Facility at the Scripps Institute of Oceanography for her scanning electron microscopy expertise, and Ryan Maloney and William Bouvier for their assistance with sample preparation.

References

1. Leidheiser, H.; Wang, W.; Igetoft, L. Prog Org Coat 1983, 11, 19.
2. Koehler, E. L. Corrosion 1984, 40, 5.
3. Wicks, Z. W., Jr.; Jones, F. N.; Pappas, S. P. Organic Coatings Science and Technology; Wiley-Interscience: New York, 1999.
4. Hamade, R. F.; Dillard, D. A. Int J Adhes Adhes 2005, 25, 147.
5. Malik, A. U.; Andijani, I.; Ahmed, S.; Al-Muaili, F. Desalination 2002, 150, 247.
6. Worthingham, R.; Cetiner, M. Proceedings of the International Pipeline Conference; American Society of Mechanical Engineers: New York, 2004; p 59.
7. Varughese, K.; Edmondson, S. J Prot Coat Linings 2006, 23, 40.
8. Xu, C.; Ramani, K.; Kumar, G. Int J Adhes Adhes 2002, 22, 187.
9. Gauthier, M.; Eisenberg, A. Macromolecules 1989, 22, 3756.
10. Ajji, A. Polym Eng Sci 1995, 35, 64.
11. Leewajanakul, P.; Pattanaolarn, R.; Ellis, J. W.; Nithitanakul, M.; Grady, B. P. J Appl Polym Sci 2003, 89, 620.
12. Love, C. T.; Xian, G.; Karbhari, V. M. Prog Org Coat 2007, 60, 287.
13. Bose, S.; Pandey, R.; Kulkarni, M. B.; Mahanwar, P. A. J Thermoplast Compos Mater 2005, 18, 393.
14. Wong, T. L.; Barry, C. M.; Orroth, S. A. J Vinyl Additive Technology 1999, 5, 235.
15. Stamhuis, J. E. Polym Compos 1988, 9, 72.
16. Osman, M. A.; Atallah, A. Macromol Rapid Commun 2004, 25, 1540.
17. Feldman, D. J Polym Environ 2001, 9, 49.
18. Murphy, J. Additives for Plastics Handbook; Elsevier Advanced Technology: Oxford, 1996.
19. Radosta, J. A.; Trivedi, N. C. In Handbook of Fillers and Reinforcements for Plastics; Katz, H. S.; Milewski, J. V., Eds.; Van Nostrand Reinhold: New York, 1978; Chapter 9.
20. Ferrigno, T. H.; Taranto, M. In Handbook of Fillers and Reinforcements for Plastics; Katz, H. S.; Milewski, J. V., Eds.; Van Nostrand Reinhold: New York, 1978; Chapter 9.
21. Othman, N.; Ismail, H.; Mariatti, M. Polym Degrad Stab 2006, 91, 1761.
22. Love, C. T.; Karbhari, V. Presented at the American Society for Composites Meeting, September 17–20, Dearborn, MI, 2006.
23. Sofian, N. M.; Rusu, M.; Neagu, R.; Neagu, E. J Thermoplast Compos Mater 2001, 14, 20.

24. Ray, S.; Easteal, A. J. Mater Manufacturing Process 2007, 22, 741.
25. Love, C. T.; Xian, G.; Karbhari, V. J Appl Polym Sci 2007, 104, 331.
26. Standard Test Method for Tensile Properties of Plastics; ASTM D 638–99; American Society for Testing and Materials: West Conshohocken, PA, 1999.
27. Standard Test Method for Pull-Off Strength of Coatings Using Portable Adhesion Testers; ASTM D 4551–02; American Society for Testing and Materials: West Conshohocken, PA, 2002.
28. Standard Test Methods for Cathodic Disbonding of Pipeline Coatings; ASTM G8–96; American Society for Testing and Materials: West Conshohocken, PA, 2003.
29. Steinsmo, U.; Skar, J. I. Corrosion 1994, 50, 934.
30. Li, J. X.; Hiltner, A.; Baer, E. J Appl Polym Sci 1994, 52, 269.
31. He, D.; Jiang, B. J Appl Polym Sci 1993, 49, 617.
32. Golam, M. N. Polym Compos 1986, 7, 176.
33. Karrad, S.; Lopez Cuesta, J. M.; Crespy, A. J Mater Sci 1998, 33, 453.
34. Halpin, J. J Compos Mater 1969, 3, 732.
35. Lewis, T. B.; Nielson, L. E. J Appl Polym Sci 1970, 14, 1449.
36. Bigg, D. M. Polym Compos 1987, 8, 115.
37. Othman, N.; Ismail, H.; Jaafar, M. Polym-Plast Technol Eng 2004, 43, 713.
38. Li, J. X.; Silverstein, M.; Hiltner, A.; Baer, E. J Appl Polym Sci 1994, 52, 255.
39. Suwanprateeb, J.; Tiemprateeb, S.; Kangwantrakool, S.; Hemachandra, K. J Appl Polym Sci 1998, 70, 1717.
40. Lipatov, Y. S.; Rosovitsky, V. F.; Babich, B. V.; Kvitka, N. A. J Appl Polym Sci 1980, 25, 1029.
41. Kalfoglou, N. K. J Appl Polym Sci 1986, 32, 5247.
42. Roy, D.; Simon, G. P.; Forsyth, M. Polym Eng Sci 2002, 42, 781.
43. Chiang, M. Y. M.; Fernandez-Garcia, M. J Appl Polym Sci 2003, 87, 1436.
44. Funke, W. J Oil Colour Chem Assoc 1985, 68, 229.
45. Harun, M. K.; Marsh, J.; Lyon, S. B. Prog Org Coat 2005, 54, 317.